

## Computer-aided approach for modelling of FG cylindrical shell sandwich with ring supports

Muzamal Hussain<sup>\*1</sup>, Muhammad Nawaz Naeem<sup>1</sup>, Muhammad Shabaz Khan<sup>1</sup> and Abdelouahed Tounsi<sup>2,3</sup>

<sup>1</sup>Department of Mathematics, Govt. College University Faisalabad, 38000, Faisalabad, Pakistan

<sup>2</sup>Materials and Hydrology Laboratory, University of Sidi Bel Abbes, Algeria Faculty of Technology, Civil Engineering Department, Algeria

<sup>3</sup>Department of Civil and Environmental Engineering, King Fahd University of Petroleum & Minerals, 31261 Dhahran, Eastern Province, Saudi Arabia

(Received January 12, 2020, Revised April 4, 2020, Accepted April 10, 2020)

**Abstract.** In this paper, the shell material has been taken as functionally graded material and their material quantity is located by the exponential volume fraction law. Moreover, the impact of ring supports around the shell circumference has been examined for their various positions along the shell axial length. These rings support restraints the radial displacement in the transverse direction. While the axial modal deformation functions have been estimated by characteristic beam functions and nature of materials used for construction of cylindrical shells. The fundamental natural frequency of cylindrical shell of parameter versus ratios of length- and height-to-radius for a wide range has been reported and investigated through the study. In addition, by increasing height-to-radius ratio resulting frequencies also increase and frequencies decrease on ratio of length-to-radius. Though the trends of frequency values of both ratios are converse to each other with three different boundary conditions. Also it is examined the position of ring supports with length-to radius ratio, height-to-radius ratio and varying the exponent of volume fraction. MATLAB software package has been utilized for extracting shell frequency spectra. The obtained results are confirmed by comparing with available literature.

**Keywords:** Galerkin's method; Lagrangian functional; ring supports; MATLAB; CSs

### 1. Introduction

The shells are basic parts in structuring different devices in engineering and technology and so on. In the seventeenth century, a thin pressure vessel in the form of a cylinder was structured and extended for industrial aims during the period: 1745-50. Investigation of vibrations for cylindrical shells was introduced by Sophie Germaine in 1821. After her research, this problem was studied by Rayleigh (1884) in the last years of the nineteenth century. Firstly, Love (1888) presented the Kirchhoff's hypotheses for plates. After that this theory became a foundation stage for building new ones by changing physical terms expressions. More than one type of materials is used to structure the functionally graded materials (FGMs) by some material manufacturing law and their physical properties vary from one surface to the other surface.

In these surfaces, one has highly heat resistance property while other may preserve great dynamical perseverance and differs mechanically and physically in regular manner from one surface to other surface, making them of dual physical appearance. All these materials have changeable outer and inner sides and their physical properties greatly differ from each other (Suresh and Mortensen 1997, Koizumi 1997).

These materials are organized by various techniques and their applications are seen in dynamical elements such as plates, beams and shells. Moreover, they are also observed in space crafts, nuclear reactors and missiles technology etc. Greif and Chung (1975) studies the vibrations of cylindrical shells for number of edge conditions with many mid-way supports between boundaries and applied the Rayleigh- Ritz formulation. Loy and Lam (1997) investigated shell vibrations with ring supports that restricted the motion of cylindrical shells in the transverse direction. This influence was inducted by the polynomial functions. Xiang *et al.* (2002) formed some closed form solution functions for studying vibrations of cylindrical shells (CSs). The mid-way ring supports were clamped around the shells. Fundamental frequencies with different parameters have been investigated with wave propagation approach. Mehar *et al.* (2020a) investigated the modal responses of multi-walled carbon nanotube-reinforced composite sandwich structural plate under the elevated temperature environment using a higher order polynomial kinematic model and the isoparametric finite element steps. The proposed model accuracy has been verified with experimental modal values under the influence of elevated temperature and ambient conditions. Sewall and Naumann (1968) considered the vibration analysis of CSs based on analytical and experimental methods. The shells were strengthened with longitudinal stiffeners. Sharma (1974) analyzed vibration frequencies circular cylinder with using the Rayleigh - Ritz formulation and made comparisons of his results with some experimental ones. Asghar *et al.* (2019) conducted the

\*Corresponding author, Ph.D.

E-mail: muzamal45@gmail.com,  
muzamalhussain@gcuf.edu.pk

vibration of nonlocal effect for double-walled carbon nanotubes using wave propagation approach. Many material parameters are varied for the exact frequencies of many indices of double-walled carbon nanotubes. Najafizadeh and Isvandzibaei (2009) presented the study of the vibration of thin cylindrical shells with ring supports made of a functionally gradient material (FGM) composed of stainless steel and nickel. Material properties are graded in the thickness direction of the shell according to volume fraction power law distribution. Effects of boundary conditions and ring support on the natural frequencies of the FGM cylindrical shell are studied. The cylindrical shells have ring supports which are arbitrarily placed along the shell and which imposed a zero lateral deflection. Chung *et al.* (1981) investigated the vibrations of fluid filled CSs and presented an analysis of experimental and analytical investigation. Goncalves and Batista (1987) gave an analytical investigation of cylindrical shell partially filled and submerged in a fluid. Recently, some researchers have done their research in concrete construction (Thomé *et al.* 2006, Meftah *et al.* 2006, Yaman *et al.* 2006, Gasser 2007). Sedighi *et al.* (2011) presented the new analytical work on the well-known preload nonlinearity using the innovative equivalent function (EF). The nonlinear vibration of cantilever beam with nonlinear boundary condition in the presence of preload spring with cubic nonlinearity is studied. The powerful analytical method, called He's Parameter Expanding Method (HPEM) is used to obtain the exact solution of dynamic behavior of the mentioned system. Fatahi-Vajari *et al.* (2019) studied the vibration of single-walled carbon nanotubes based on Galerkin's and homotopy method. This work analyses the nonlinear coupled axial-torsional vibration of single-walled carbon nanotubes (SWCNTs) based on numerical methods. Two-second order partial differential equations that govern the nonlinear coupled axial-torsional vibration for such nanotube were derived. Jiang and Olson (1994) recommended the characteristics of analysis of stiffened shell using finite element method to diminish large computational efforts which are required in the conventional finite element analysis. Sharma *et al.* (2019) studied the functionally graded material using sigmoid law distribution under hygrothermal effect. The Eigen frequencies are investigated in detail. Frequency spectra for aspect ratios have been depicted according to various edge conditions. Mehar *et al.* (2019) reported the buckling load parameters of the graded nanotube sandwich structure under the influence of uniform thermal loading. The corresponding properties of the graded nanotube sandwich evaluated via the extended rule of mixture including temperature dependent properties of each constituent. The nanotube structural model derived mathematically using a higher-order polynomial displacement to maintain the required shear stress continuity and thermal distortion via Green-Lagrange strain. Swaddiwudhpong *et al.* (1995) conducted the vibrations of cylindrical shells (CSs) using Ritz polynomials. The axial modal deformation displacements with various boundary conditions were investigated for any number of intermediate supports. The procedure was easy for computer programming for various

combinations of boundary conditions. Alazzawy and Jweeg (2010) studied the free vibration solution for laminated simply supported closed cylindrical shells. This solution is obtained using general third shell theory (GTT). Also the critical in-plane fatigue load is studied and the required equilibrium equations are developed, the effects of tension or compression in-plane load on the natural frequencies are discussed also. Mehar *et al.* (2020b) studied the thermal frequency of the graded nanotube-reinforced composite structure embedded with shape memory alloy (SMA) fiber first time numerically using a micromechanical multiscale finite element material model. The smart nanotube-reinforced composite structure has been formulated through the higher-order kinematics including the shear deformations. Hussain and Naeem (2018a) used Donnell's shell model to calculate the dimensionless frequencies for two types of single-walled carbon nanotubes. The frequency influence was observed with different parameters. Salamat and Sedighi (2017) investigated the free and forced vibration of simply-supported single-walled carbon nanotube under the moving nanoparticle by considering nonlocal cylindrical shell model. To validate the theoretical results, modal analysis of nanotube is conducted using ANSYS commercial software. Excellent agreement is exhibited between the results of two different methods. Furthermore, the dynamic response of SWCNT under moving nanoparticle is also studied. Hussain and Naeem (2017) examined the frequencies of armchair tubes using Flügge's shell model. The effect of length and thickness-to-radius ratios against fundamental natural frequency with different indices of armchair tube was investigated. Mehar *et al.* (2016) investigated the free vibration behavior of functionally graded carbon nanotube reinforced composite plate under elevated thermal environment. The carbon nanotube reinforced composite plate has been modeled mathematically using higher order shear deformation theory. The material properties of carbon nanotube reinforced composite plate are assumed to be temperature dependent and graded in the thickness direction using different grading rules. Jweeg and Alazzawy (2007) developed the transient solutions for laminated simply supported closed cylindrical shells subjected to a uniform dynamic pressure at the outer surface of the cylinder. Rectangular pulse, triangular pulse, sinusoidal pulse and (ramp-constant) load-time varying functions are studied and the required equilibrium equations are developed. Hussain *et al.* (2017) demonstrated an overview of Donnell theory for the frequency characteristics of two types of SWCNTs. Fundamental frequencies with different parameters have been investigated with WPA. Sedighi *et al.* (2017) provided the static and dynamic pull-in behavior of nano-beams resting on the elastic foundation based on the nonlocal theory which is able to capture the size effects for structures in micron and sub-micron scales. For this purpose, the governing equation of motion and the boundary conditions are driven using a variational approach. Wang *et al.* (1997) scrutinized the vibrations of a ring-stiffened CSs using Ritz polynomial functions. Materials of both shells and rings were of isotropic nature. These shells are stiffened with isotropic rings having three types of locations on the

shell outer surface. To increase the stiffness of CSs was stabilized by ring-stiffeners. Isotopic materials are the constituents of these rings. Sharma *et al.* (1998) determined frequencies of composite cylindrical shells containing fluid. They estimated the axial modal deformations by the Fourier series of trigonometric functions. Mehar and Panda (2016) investigated the nonlinear free vibration behavior of functionally graded carbon nanotube reinforced composite flat panel using temperature dependent material properties for different grading. The carbon nanotube reinforced composite flat panel model has been developed mathematically using the higher-order shear deformation theory and Green-Lagrange nonlinearity. Wang and Lai (2000) presented simple approach for the evaluation of eigen-frequencies of cylindrical shells. The numerical process adopted by them was alike the wave propagation approach (WPA). Ergin and Temarel (2002) did a vibration study of cylindrical shells. The shells lied in a horizontal direction and contained fluid and submerged in it. Zhang (2002) studied vibrations of CSs submerged in a fluid. It was seen that the fluid factor impressed vibration shell frequencies to a significant limit. Najafzadeh and Isvandzibaei (2007) applied ring supports to CSs for vibration analysis of along the tangential direction and founded their research on angular deformation theory of higher order. The angular deformation shell theory of third order was used for shell equations and determined the effects of constituent volume fractions, shell configurations on the shell vibrations. FG material parameters were changed step by step. Recently, Hussain and Naeem (2019a, b, c, d, 2020a) and performed the vibration of SWCNTs based on wave propagation approach and Galerkin's method. They investigated many physical parameters for the rotating and non-rotating vibrations of armchair, zigzag and chiral indices. Moreover, the mass density effect of single walled carbon nanotubes with in-plane rigidity have been calculated for zigzag and chiral indices. Shah *et al.* (2009) and Sofiyev and Avcar (2010) studied stability of CSs based on Rayleigh - Ritz and Galerkin technique using elastic foundations. The structures of cylindrical shell were tackled under the exponential law and axial load. Naeem *et al.* (2013) conducted the vibrational behavior of submerged FG-CSs. The problem of submerged cylindrical shells is frequently met where fluid envelopes a structure. The present problem consists of a cylindrical shell submerged in a fluid and surrounded by ring supports. There is no evidence found where this problem has not been studied earlier. Ansari *et al.* (2015) performed nonlocal model for the frequencies of multi-walled carbon nanotubes with small effects subject to various boundary conditions using Rayleigh-Ritz technique. The governing equation was formulated based on Flügge's and nonlocal shell theory. Some new resonant frequencies are identified with the association of vibrational modes and circumferential modes into shell model. Mehar *et al.* (2017a) studied the nonlinear eigen frequency response of the functionally graded single-walled carbon nanotube reinforced sandwich structure numerically considering the Green- Lagrange nonlinear strain under uniform thermal environment. The mathematical model of the sandwich plate has been derived

using the simple higher-order shear deformable kinematics including the temperature dependent properties of each constituent. Hussain and Naeem (2018) used Donnell's shell model to calculate the dimensionless frequencies or two types of single-walled carbon nanotubes. The frequency influence was observed with different parameters. Recently, many researchers used different methods at nano level (Bilouei *et al.* 2016, Golabchi *et al.* 2018, Lal and Markad 2018, Mousavi *et al.* 2019, Loghman *et al.* 2017, Zamani *et al.* 2017, Batou *et al.* 2019, Salah *et al.* 2019, Ayat *et al.* 2018, Jamali *et al.* 2019, Behera and Kumari 2018, Narwariya *et al.* 2018, Rezaiee-Pajand *et al.* 2018, Yazdani and Mohammadimehr 2019, Esmaeili and Andalibia 2019, Mehar and Panda 2019).

According to our knowledge, up to now little is known about the vibration analyses of ring supports with exponential volume fraction laws and moreover, the influence of length-to-radius ratio, thickness-to-radius ratio and varying of exponents of volume fraction have not been investigated for FG-CS based on Galerkin's technique. Many material researchers calculated the frequency of CNTs using different techniques (Mehar and Panda 2017a, b, c, d, Mehar and Panda 2018, Mehar *et al.* 2017c, d, Mehar *et al.* 2018), for example, multiscale modeling approach (Mehar and Panda 2019, Mehar *et al.* 2019).

The proposed model are quite straightforward for the vibrational analysis of these structures of CSs. The shell are stabilized by ring supports to increase the stiffness and strength. Isotopic materials are the constituents of these rings. A large use of shell structures in practical applications makes their theoretical analysis an important field of structural dynamics. Since a shell problem is a physical one, so their vibrational behaviors are distorted by variations of physical and material parameters. Effects of different parameters for ratios of length- and height-to-radius versus fundamental natural frequencies are investigated. In this paper, utilizing the Love shell theory with exponential volume fraction laws for the CSs vibrations provides a governing equation. It is also exhibited the effect of frequencies by varying the positions of ring supports and ratios of length- and- height-to-radius. Throughout the computation, it is observed that the frequency behavior for the boundary conditions follow as; clamped-clamped (C-C), simply supported-simply supported (SS-SS) frequency curves are higher than that of clamped-free (C-F) curves. Also the Love shell model based on the Galerkin's method for estimating fundamental natural frequency has been developed to converge more quickly than other methods and models. In addition, by increasing the value of height-to-radius ratio resulting frequencies also increase and frequencies decrease on increasing the ratio of length-to-radius ratio. The presented vibration modeling and analysis of CSs may be helpful especially in applications such as oscillators and in non-destructive testing. To elude any complications which may risk a physical system their analytical investigation is done. The shells are supported by isotropic ring-supports.

## 2. Theoretical formation

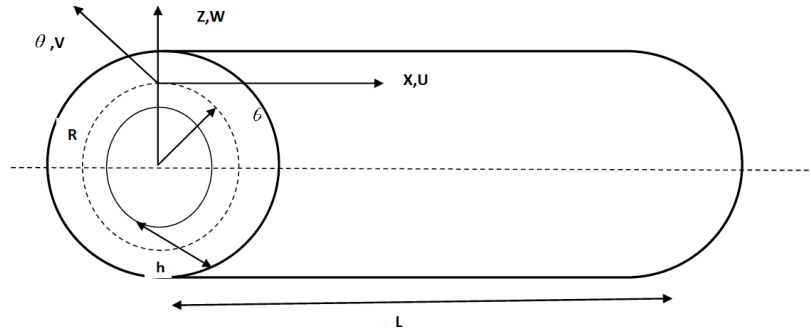


Fig. 1 Geometry of shell

Geometrical structure of a cylinder is sketched in Fig. 1. Strain energy  $U$  for FG-CS (Naeem *et al.* 2013).

$$U = \frac{1}{2} \int_0^L \int_0^{2\pi} [\alpha]^T [\alpha] [S] R d\theta dx \quad (1)$$

where

$$\{\alpha\}^T = \{e_1 \quad e_2 \quad \lambda \quad \kappa_1 \quad \kappa_2 \quad 2\tau\} \quad (2)$$

whereas  $(e_1, e_2, \gamma)$  and  $(\kappa_1, \kappa_2, \tau)$  are referenced as surface curvature and surface strains

$$[S] = \begin{pmatrix} A_{11} & A_{12} & 0 & B_{11} & B_{12} & 0 \\ A_{12} & A_{22} & 0 & B_{12} & B_{22} & 0 \\ 0 & 0 & A_{66} & 0 & 0 & B_{66} \\ B_{11} & B_{12} & 0 & D_{11} & D_{12} & 0 \\ B_{12} & B_{22} & 0 & D_{12} & D_{22} & 0 \\ 0 & 0 & B_{66} & 0 & 0 & D_{66} \end{pmatrix} \quad (3)$$

where the membrane  $(A_{ij})$ , coupling  $(B_{ij})$  and flexural  $(D_{ij})$  stiffness are expressed as

$$\left. \begin{aligned} A_{ij} &= \int_{-\frac{h}{2}}^{\frac{h}{2}} Q_{ij} dz \\ B_{ij} &= \int_{-\frac{h}{2}}^{\frac{h}{2}} z Q_{ij} dz \\ D_{ij} &= \int_{-\frac{h}{2}}^{\frac{h}{2}} z^2 Q_{ij} dz \end{aligned} \right\} \quad (4)$$

For isotropic CSs the coupling stiffness  $B_{ij}$  condensed to zero when its material is isotropic and does not become zero when a cylindrical shell is structured from composite or laminated or functionally graded material.

$Q_{ij}$  is reduced stiffness for isotropic materials with conjunction of  $E$  and  $\nu$  are written as

$$\left. \begin{aligned} Q_{11} &= Q_{22} = \frac{E}{1-\nu^2} \\ Q_{12} &= \frac{\nu E}{1-\nu^2} \\ Q_{66} &= \frac{E}{2(1+\nu)} \end{aligned} \right\} \quad (5)$$

Strain energy modified form is achieved after putting

$\{\alpha\}^T$  and  $[S]$  in Eq. (1)

$$U = \frac{1}{2} \int_0^L \int_0^{2\pi} \left\{ A_{11} e_1^2 + A_{22} e_2^2 + 2A_{12} e_1 e_2 + A_{66} \gamma^2 \right. \\ \left. + 2B_{11} e_1 \kappa_1 + 2B_{12} e_1 \kappa_2 + 2B_{12} e_2 \kappa_1 + 2B_{22} e_2 \kappa_2 \right. \\ \left. + 4B_{66} \gamma \tau + D_{11} \kappa_1^2 + D_{22} \kappa_2^2 + 2D_{12} \kappa_1 \kappa_2 \right. \\ \left. + 4D_{66} \tau^2 \right\} R d\theta dx \quad (6)$$

## 2.1 Relationship of strain-displacement expressions

With advancements in study of shell problem, new shell theories were developed and used to do vibration analysis of cylindrical shell problems. There found minute differences in numerical results when different shell theories were utilized. Applying Love shell theory, strain-displacement expressions are stated as

$$\{e_1, e_2, \gamma\} = \left\{ \frac{\partial u}{\partial x}, \frac{1}{R} \left( \frac{\partial v}{\partial \theta} + w \right), \frac{\partial v}{\partial x} + \frac{1}{R} \frac{\partial u}{\partial \theta} \right\} \quad (7)$$

Similarly relations for curvature - displacement for  $\kappa_1, \kappa_2, \tau$  are written as:

$$\left\{ \kappa_1, \kappa_2, \tau \right\} = \left\{ -\frac{\partial^2 w}{\partial x^2}, -\frac{1}{R^2} \left( \frac{\partial^2 w}{\partial \theta^2} - \frac{\partial v}{\partial \theta} \right), -\frac{1}{R} \left( \frac{\partial^2 w}{\partial x \partial \theta} - \frac{\partial v}{\partial x} \right) \right\} \quad (8)$$

On substitution of the expressions (7) and (8) in the relation (6), the strain energy  $U$  in modified form can be elaborated as

$$U = \frac{1}{2} \int_0^L \int_0^{2\pi} \left[ A_{11} \left( \frac{\partial u}{\partial x} \right)^2 + A_{22} \frac{1}{R^2} \left( \frac{\partial v}{\partial \theta} + w \right)^2 \right. \\ \left. + 2A_{12} \frac{1}{R} \frac{\partial u}{\partial x} \left( \frac{\partial v}{\partial \theta} + w \right) + A_{66} \left( \frac{\partial v}{\partial \theta} + \frac{1}{R} \frac{\partial u}{\partial x} \right)^2 \right. \\ \left. - 2B_{11} \left( \frac{\partial u}{\partial x} \right) \left( \frac{\partial^2 w}{\partial x^2} \right) - 2B_{12} \frac{1}{R^2} \left( \frac{\partial u}{\partial x} \right) \left( \frac{\partial^2 w}{\partial \theta^2} - \frac{\partial v}{\partial \theta} \right) \right. \\ \left. - 2B_{12} \frac{1}{R} \left( \frac{\partial v}{\partial \theta} + w \right) \left( \frac{\partial^2 w}{\partial x^2} \right) - 2B_{22} \frac{1}{R^3} \left( \frac{\partial v}{\partial \theta} + w \right) \right. \\ \left. \left( \frac{\partial^2 w}{\partial \theta^2} - \frac{\partial v}{\partial \theta} \right) - 4B_{66} \frac{1}{R} \left( \frac{\partial v}{\partial \theta} + \frac{1}{R} \frac{\partial u}{\partial x} \right) \right. \\ \left. \left( \frac{\partial^2 w}{\partial x \partial \theta} - \frac{3}{4} \frac{\partial v}{\partial x} + \frac{1}{4R} \frac{\partial u}{\partial \theta} \right) + D_{11} \left( \frac{\partial^2 w}{\partial x^2} \right)^2 \right. \\ \left. + D_{22} \left( \frac{\partial^2 w}{\partial \theta^2} - \frac{\partial v}{\partial \theta} \right)^2 + 2D_{12} \left( \frac{\partial^2 w}{\partial x \partial \theta} - \frac{3}{4} \frac{\partial v}{\partial x} + \frac{1}{4R} \frac{\partial u}{\partial \theta} \right) \left( \frac{\partial^2 w}{\partial \theta^2} - \frac{\partial v}{\partial \theta} \right) \right] R d\theta dx$$

$$+ \frac{D_{22}}{R^4} \left( \frac{\partial^2 w}{\partial \theta^2} - \frac{\partial v}{\partial \theta} \right)^2 + 2D_{12} \frac{1}{R^2} \left( \frac{\partial^2 w}{\partial x^2} \right) \left( \frac{\partial^2 w}{\partial \theta^2} - \frac{\partial v}{\partial \theta} \right) + 4D_{66} \frac{1}{R^2} \left( \frac{\partial^2 w}{\partial x \partial \theta} - \frac{3}{4} \frac{\partial v}{\partial x} + \frac{1}{4R} \frac{\partial u}{\partial \theta} \right)^2 R dx d\theta \quad (9)$$

Similarly kinetic energy for a CSs doing vibration is written as

$$K = \frac{1}{2} \iint_0^{2\pi L} \rho_T \left[ \left( \frac{\partial u}{\partial t} \right)^2 + \left( \frac{\partial v}{\partial t} \right)^2 + \left( \frac{\partial w}{\partial t} \right)^2 \right] R dx d\theta \quad (10)$$

The mass density relation  $\rho_T$  is expressed as

$$\rho_T = \int_{-\frac{h}{2}}^{\frac{h}{2}} \rho dz \quad (11)$$

With the coalescence energies (strain and kinetic), the Lagrangian functional can be obtained can be given as (Sodel 1981)

$$\Pi = K - U \quad (12)$$

## 2.2 Shell dynamical equations

When a shell problem is formed in the integral form, it can be solved by applying the Rayleigh-Ritz method. The shell governing equations are formed in a system of PDEs in three unknown displacement functions. These equations are framed from the Lagrangian functional (12) with process of variation. So application of the Hamiltonian variational principle, the governing equations are given by

$$A_{11} \frac{\partial^2 u}{\partial x^2} + \frac{A_{66}}{R^2} \frac{\partial^2 u}{\partial \theta^2} + \left( \frac{A_{12} + A_{66}}{R} + \frac{B_{11} + 2B_{66}}{R^2} \right) \frac{\partial^2 v}{\partial x \partial \theta} + \frac{A_{12}}{R} \frac{\partial w}{\partial x} - B_{11} \frac{\partial^3 w}{\partial x^3} - \left( \frac{B_{12} + 2B_{66}}{R^2} \right) \frac{\partial^3 w}{\partial x \partial \theta^2} = \rho_i \frac{\partial^2 u}{\partial t^2}, \quad (13a)$$

$$\left( \frac{A_{12} + A_{66}}{R} + \frac{B_{11} + 2B_{66}}{R^2} \right) \frac{\partial^2 u}{\partial x \partial \theta} + \left( \frac{A_{22}}{R^2} + \frac{2B_{66}}{R^3} + \frac{D_{22}}{R^4} \right) \frac{\partial^2 v}{\partial \theta^2} + \left( A_{66} + \frac{4B_{66}}{R^2} + \frac{4D_{66}}{R^2} \right) \frac{\partial^2 v}{\partial x^2} + \left( \frac{A_{22}}{R^2} + \frac{B_{22}}{R^3} \right) \frac{\partial w}{\partial \theta} - \left( \frac{B_{22}}{R^3} + \frac{D_{22}}{R^4} \right) \frac{\partial^3 w}{\partial \theta^3} - \left( \frac{B_{12} + 2B_{66}}{R} + \frac{D_{12} + 4D_{66}}{R^2} \right) \frac{\partial^3 w}{\partial x^2 \partial \theta} = \rho_i \frac{\partial^2 v}{\partial t^2}, \quad (13b)$$

$$\frac{A_{12}}{R} \frac{\partial u}{\partial x} - B_{11} \frac{\partial^3 u}{\partial x^3} - \left( \frac{B_{11} + 2B_{66}}{R^2} \right) \frac{\partial^3 u}{\partial x \partial \theta^2} + \left( \frac{A_{22}}{R^2} + \frac{B_{22}}{R^3} \right) \frac{\partial v}{\partial \theta} - \left( \frac{B_{22}}{R^3} + \frac{D_{22}}{R^4} \right) \frac{\partial^3 v}{\partial \theta^3} - \left( \frac{B_{12} + 2B_{66}}{R} + \frac{D_{12}}{R^2} + \frac{4D_{66}}{R^2} \right) \frac{\partial^3 v}{\partial x^2 \partial \theta} + \frac{A_{22}}{R^2} w - \frac{B_{12}}{R} \frac{\partial^2 w}{\partial x^2} - \frac{B_{22}}{R^3} \frac{\partial^2 w}{\partial \theta^2} + \left( \frac{D_{22}}{R^4} \right) \frac{\partial^4 w}{\partial \theta^4} + D_{11} \frac{\partial^4 w}{\partial x^4} + \left( \frac{2D_{12}}{R^2} + \frac{4D_{66}}{R^2} \right) \frac{\partial^4 w}{\partial x^2 \partial \theta^2} = -\rho_i \frac{\partial^2 w}{\partial t^2} \quad (13c)$$

## 2.3 The Galerkin technique

Over the past several years vibration of nanostructures of various configurations and boundary conditions have been extensively studied (Hussain *et al.* 2018a, Hussain *et al.* 2018b, Hussain *et al.* 2018c, Hussain and Naeem 2018b, Hussain *et al.* 2019a, Hussain *et al.* 2019b, Hussain *et al.* 2020a, Hussain and Naeem 2020b, Asghar *et al.* 2020, Hussain *et al.* 2020b, c, d, e, f, g, Taj *et al.* 2020a, Taj *et al.* 2020a, b, c). Many material researchers has used various methods to solve PDEs (Wuite *et al.* 2005). Closed form functions exist for solutions of shell motion equations for some types of edge conditions. For rest of boundary conditions, the numerical solutions are obtained by approximate methods. Galerkin's method is made to extract approximate solution of shell controlling equations because these techniques provide results robustly with sufficient accuracy. This method is appropriate, straightforward to extract the shell vibration frequencies. Differential equations are generated involving the three dependent variables. Boundary conditions existing at the shell ends are met by these functions. For solving the shell problem, first the special variables  $x$ ,  $\theta$  and temporal variable  $t$  are split. For this purpose the following modal displacement expressions for the deformation functions:  $u$ ,  $v$  and  $w$  are presupposed as:

$$u(x, \theta, t) = \frac{d\psi}{dx} A_m \sin n\theta \cos \omega t \quad (14)$$

$$v(x, \theta, t) = \psi(x) B_m \cos n\theta \cos \omega t \quad (15)$$

$$w(x, \theta, t) = \psi(x) C_m \prod_{i=1}^k (x - a_i)^{b_i} \sin n\theta \cos \omega t \quad (16)$$

Where the parameters  $A_m$ ,  $B_m$  and  $C_m$  in the relations (14)-(16) represents the vibration in the  $x$ ,  $\theta$  and  $z$  directions correspondingly.  $\psi(x)$  signifies the unknown axial deformation function that fulfills the end conditions stated at two shell ends. The position of  $i$ th ring support is denoted by  $a_i$  from the  $x=0$  along the longitudinal direction. In Eq. (16),  $k$  represents number of ring supports.  $b_i$  Possesses the value 1 when a ring support is linked and is zero when no support is held up. Making substitutions of the expressions for the deformation displacement functions from Eq. (14), (15), (16) into Eq. (13a), (13b), (13c) with their corresponding derivatives, by taking  $b_i=1$  and multiplying with  $\frac{d\psi}{dx}$ ,  $\psi(x)$  and  $\psi(x)(x-a)$  respectively. We attained an

equation after integrating  $x$  from 0 to  $L$

$$\left( A_{11} I_1 - n^2 \frac{A_{66}}{R^2} I_2 \right) A_m - n \left( \frac{A_{12} + A_{66}}{R} + \frac{B_{12} + 2B_{66}}{R^2} \right) I_2 B_m + \left[ \frac{A_{12}}{R} (I_6 + I_7) - B_{11} (I_8 + 3I_9) + n^2 \frac{B_{12} + 2B_{66}}{R^2} (I_6 + I_7) \right] C_m = -\omega^2 \rho h I_2 A_m + n \left( \frac{A_{12} + A_{66}}{R} + \frac{B_{12} + 2B_{66}}{R^2} \right) I_3 A_m + \left[ \left( A_{66} + \frac{3B_{66}}{R} + \frac{4D_{66}}{R^2} \right) I_3 - n^2 \left( \frac{A_{22}}{R^2} + \frac{2B_{22}}{R^3} + \frac{D_{22}}{R^4} \right) I_4 \right] B_m + \quad (16a)$$

$$\begin{bmatrix} n\left(\frac{A_{22}}{R^2} + \frac{B_{22}}{R^3}\right)I_{10} + n^3\left(\frac{B_{22}}{R^3} + \frac{D_{22}}{R^4}\right)I_{10} \\ -n\left(\frac{B_{12} + 2B_{66}}{R} + \frac{D_{12} + 4D_{66}}{R^2}\right)(I_{11} + 2I_{12}) \end{bmatrix} C_m = -\omega^2 \rho h I_4 B_m \quad (16b)$$

$$\begin{aligned} & \left( -\frac{A_{12}}{R} I_{18} + B_{11} I_{19} - n^2 \frac{B_{12} + 2B_{66}}{R^2} I_{18} \right) A_m \\ & + \left[ n\left(\frac{A_{22}}{R^2} + \frac{B_{22}}{R^3}\right)I_{10} + n^3\left(\frac{B_{22}}{R^3} + \frac{D_{22}}{R^4}\right)I_{10} \right. \\ & \left. - n\left(\frac{B_{12} + 2B_{66}}{R} + \frac{D_{12} + 4D_{66}}{R^2}\right)I_{18} \right] B_m \\ & + \left[ -\frac{A_{22}}{R^2} I_3 + \frac{2B_{12}}{R} (I_{14} + 2I_{15}) - 2n^2 \frac{B_{22}}{R^3} I_{13} \right. \\ & \left. - D_{11} (I_{16} + 4I_{17}) + 2n^2 \frac{D_{12} + 2D_{66}}{R^2} (I_{14} + 2I_{15}) - \frac{D_{22}}{R^4} I_{13} \right] C_m \\ & = -\omega^2 \rho h I_{13} C_m \end{aligned} \quad (16c)$$

The integral term are tabulated in Appendix-I.

Making the arrangement of terms in the Eqs. (16a)-(16c), the shell frequency equation framed in the eigenvalue form as below (Dong 1977)

$$\begin{cases} \hat{\lambda}_{11} A_m + \hat{\lambda}_{12} B_m + \hat{\lambda}_{13} C_m = -\omega^2 \rho h A_m I_2 \\ \hat{\lambda}_{21} A_m + \hat{\lambda}_{22} B_m + \hat{\lambda}_{23} C_m = -\omega^2 \rho h B_m I_4 \\ \hat{\lambda}_{31} A_m + \hat{\lambda}_{32} B_m + \hat{\lambda}_{33} C_m = -\omega^2 \rho h C_m I_{13} \end{cases} \quad (17)$$

Here terms  $\hat{\lambda}_{ij}$  ( $i, j = 1, 2, 3$ ) implicate geometrical and material quantities and are tabulated in the Appendix-I. The above equations can be arranged in matrices form as

$$\begin{pmatrix} \hat{\lambda}_{11} & \hat{\lambda}_{12} & \hat{\lambda}_{13} \\ \hat{\lambda}_{21} & \hat{\lambda}_{22} & \hat{\lambda}_{23} \\ \hat{\lambda}_{31} & \hat{\lambda}_{32} & \hat{\lambda}_{33} \end{pmatrix} \begin{pmatrix} A_m \\ B_m \\ C_m \end{pmatrix} = -\omega^2 \rho h \begin{pmatrix} I_2 & 0 & 0 \\ 0 & I_4 & 0 \\ 0 & 0 & I_{13} \end{pmatrix} \begin{pmatrix} A_m \\ B_m \\ C_m \end{pmatrix} \quad (18)$$

## 2.4 Functionally graded materials

On mixing two or more than two materials like ceramic and metal, functionally graded materials are obtained. This type of material are working in high-temperature dependence material goods. To recover the performance of the material it is circulated the functionality between the surface with high wear resistance and inside with high toughness which have material parameters:  $E_1$ ,  $E_2$ ,  $\nu_1$ ,  $\nu_2$ , and  $\rho_1$ ,  $\rho_2$ . Then the effective material quantities:  $E_{FGM}$ ,  $\nu_{FGM}$  and  $\rho_{FGM}$  are stated as (Naeem *et al.* 20130, Hussain *et al.* 2018c)

$$\begin{aligned} E_{FGM} &= \frac{[E_1 - E_2]}{\left[\frac{z}{h} + \frac{1}{2}\right]^q} + E_2, \quad \nu_{FGM} = \frac{[\nu_1 - \nu_2]}{\left[\frac{z}{h} + \frac{1}{2}\right]^q} + \nu_2, \\ \rho_{FGM} &= \frac{[\rho_1 - \rho_2]}{\left[\frac{z}{h} + \frac{1}{2}\right]^q} + \rho_2 \end{aligned} \quad (19)$$

where  $q$  known as power law index and thickness and  $z$  is

the coordinate which varies from zero to infinity. The distribution of volume fraction for all types of CSs are assumed as (Chi and Chung 2006)

$$V_f = \left[ \frac{z}{h} + \frac{1}{2} \right]^q \quad (20)$$

## 2.5 Volume fraction law

This supposition simplifies the procedure of evaluation of integrals denoting material stiffness moduli. A FG-CS consisting of two constituent materials. In these categories nickel and stainless steel are used as the interior surfaces and the exterior surface respectively, but their arrangement has profound influence on the formation of FG-CSs. The order of the FG constituent materials is reversed as category I (C-I) and category II (C-II). The volume fraction  $V_f$  are designated for CSs, respectively. Their exist a property of unity for composite material (Arshad *et al.* 2007).

$$V_f = 1 - \frac{1}{e^{\left(\frac{z}{h} + 0.5\right)^q}} \quad (21)$$

where  $e$  is natural exponent. Therefore, from these expressions, the actual fabric properties: mass density  $\rho$ , Poisson ratio  $\nu$ , and Young's modulus  $E$ , for a FG-CS are expressed as

$$\begin{aligned} E_{FGM} &= \left( 1 - \frac{1}{e^{\left(\frac{z}{h} + 0.5\right)^q}} \right) (E_1 - E_2) + E_2, \\ \nu_{FGM} &= \left( 1 - \frac{1}{e^{\left(\frac{z}{h} + 0.5\right)^q}} \right) (\nu_1 - \nu_2) + \nu_2 \\ \rho_{FGM} &= \left( 1 - \frac{1}{e^{\left(\frac{z}{h} + 0.5\right)^q}} \right) (\rho_1 - \rho_2) + \rho_2 \end{aligned} \quad (22)$$

For  $z = -h/2$ ,  $E_{FGM} = E_2$ ,  $\nu_{FGM} = \nu_2$ , and  $\rho_{FGM} = \rho_2$ ,

and for  $z = h/2$ ,

$$E_{FGM} = (E_1 - E_2)(1 - e^{-1}) + E_2, \quad \nu_{FGM} = (\nu_1 - \nu_2)(1 - e^{-1}) + \nu_2,$$

and  $\rho_{FGM} = (\rho_1 - \rho_2)(1 - e^{-1}) + \rho_2$ .

The material parameters:  $E_1$ ,  $E_2$ ,  $\nu_1$ ,  $\nu_2$ , and  $\rho_1$ ,  $\rho_2$  for constituents materials stainless steel and nickel at a temperature of 300K are given in (Arshad *et al.* 2007). Touloukian *et al.* (1967) stated the material properties  $\eta$  at high temperature environ, with temperature-dependents which is a function of temperature. In Eq. (23), the constants ( $\eta_0$ ,  $\eta_{-1}$ ,  $\eta_1$ ,  $\eta_2$ ,  $\eta_3$ ) are different for different material.

$$\eta = \eta_0 (\eta_{-1} T^{-1} + \eta_1 T + \eta_2 T^2 + \eta_3 T^3) \quad (23)$$

At temperature 300K, for stainless steel and nickel, the material properties for FG-CS are:  $E$ ,  $\nu$ ,  $\rho$  for stainless steel

Table 1 Convergence of SS-SS frequencies with frequency parameter  $\lambda = \omega R \sqrt{(1-\nu^2)\rho/E}$  (Xiang *et al.* 2002)

$n$	Method	$m$		
		1	2	3
1	Xiang <i>et al.</i> (2002)	0.0161029	0.039271	0.1098116
	Present	0.0161028	0.0392714	0.1098115

Table 2 Convergence of SS-SS frequencies (Loy *et al.* 1999)

$n$	Method	$m$				
		1	2	3	4	5
2	Loy <i>et al.</i> (1999)	2050.7	5643.3	8941.3	11416.9	13262.9
	Present	2044.7	5635.4	8932.5	11407.5	13253.2
3	Loy <i>et al.</i> (1999)	2204	4052	6633.3	9140.6	11378.8
	Present	2195	4035.5	6630.6	9135	11368.9

(SST) are  $2.0778 \times 10^{11}$  N/m<sup>2</sup>, 0.317756 and 8166 Kg/m<sup>3</sup> and nickel (Ni) are  $2.05098 \times 10^{11}$  N/m<sup>2</sup>, 0.3100, and 8900 Kg/m<sup>3</sup>. These values have been taken from references (Loy *et al.* 1999).

### 3. Results and discussion

In this paper, vibrational frequencies for functionally graded cylindrical shells are presented and analyzed. The Galerkin's method which is versatile numerical technique

Table 3 Convergence of clamped-clamped frequencies with frequency parameter  $\lambda = \omega R \sqrt{(1-\nu^2)\rho/E}$  (Xuebin 2008)

Method	$n$			
	2	3	4	5
Xuebin (2008)	0.014052	0.022726	0.042272	0.068116
Present	0.014256	0.022713	0.042215	0.06805

Table 4 Convergence of frequencies (Lam and Loy 1998) for a clamped-free isotropic CSs

$m$	method	$n$			
		3	4	5	6
1	Lam and Loy (1998)	759.9	1459.3	2360.9	3463.9
	Present	765.3	1460.2	2361.1	3464

has been used in the present study to explore the vibration characteristics of FG-CSs with ring supports. For the convergence rate of CSs, the non-dimensional frequency parameters enumerated in the current work, i.e., using Galerkin's method, are happened to be in a good consistency along with the so-called exact results furnished by (Xiang *et al.* 2002, Loy *et al.* 1999, Xuebin 2008, Lam and Loy 1998), those were established by working out with three boundary conditions as provided in Tables 1-4. The proposed model based on Galerkin's can incorporate in order to accurately predict the acquired results of material data point and the percentage difference is negligible.

Table 5 Clamped-clamped frequencies (Hz) against the circumferential wave number ( $n$ ) ( $h/R=0.002$  m,  $L/R=20$  m)

$n$	$q=0.5$			$q=1$			$q=8$		
	S-S	C-C	C-F	S-S	C-C	C-F	S-S	C-C	C-F
Category-I	1	13.213	28.292	5.41	13.142	28.141	5.382	12.95	27.73
	2	4.472	9.913	2.08	4.446	9.858	2.069	4.384	9.716
	3	4.15	5.95	3.698	4.125	5.916	3.678	4.07	5.834
	4	7.041	7.464	6.951	7.001	7.421	6.913	6.905	7.32
	5	11.253	11.369	11.223	11.191	11.306	11.162	11.036	11.15
Category -II	1	13.258	28.357	5.057	13.332	28.516	5.085	13.538	28.957
	2	4.496	9.934	2.065	4.524	9.99	2.078	4.591	10.144
	3	4.169	5.969	3.705	4.195	6.004	3.726	4.254	6.093
	4	7.056	7.48	6.961	7.096	7.524	7.001	7.2	7.633
	5	11.268	11.385	11.236	11.331	11.449	11.299	11.498	11.617

Table 6 Clamped-clamped frequencies (Hz) against axial wave mode ( $m$ ) ( $n=1$ ,  $h/R=0.002$  m,  $L/R=20$  m)

$m$	$q=0.5$			$q=1$			$q=8$		
	S-S	C-C	C-F	S-S	C-C	C-F	S-S	C-C	C-F
Category -I	1	13.213	28.292	5.052	13.142	28.141	5.025	12.95	27.73
	2	48.48	69.643	29.663	48.221	69.271	29.505	47.517	68.259
	3	97.295	120.07	74.424	96.776	119.43	74.027	95.362	117.68
	4	152.73	174.62	128.88	151.92	173.7	128.2	149.7	171.15
	5	210.48	230.33	187.53	209.36	229.11	186.52	206.3	225.75
Category -II	1	13.258	28.357	5.057	13.332	28.516	5.085	13.538	28.957
	2	48.652	69.864	29.717	48.925	70.256	29.884	49.682	71.343
	3	97.657	120.51	74.619	98.205	121.19	75.038	99.725	123.06
	4	153.32	175.35	129.29	154.19	176.31	130.02	156.57	179.03
	5	211.32	231.29	188.19	212.51	232.59	189.24	215.8	236.63

Table 7 Clamped-clamped frequencies (Hz) against length-to-radius ratio  $L/R$ 

	$L/R$	$q=0.5$			$q=1$			$q=8$		
		S-S	C-C	C-F	S-S	C-C	C-F	S-S	C-C	C-F
Category -I	1	669.14	722.53	558.9	689.44	28.141	555.92	679.37	27.73	549.02
	2	469.27	518.23	276.16	466.77	69.271	274.69	459.95	68.259	270.68
	3	152.73	215.33	69.25	151.92	119.43	68.881	149.7	117.68	67.874
	4	89.786	143.05	38.037	89.306	173.69	37.833	88.001	171.15	37.281
	5	48.48	87.567	19.497	48.221	229.1	19.393	47.517	225.75	19.11
Category -II	1	695.57	724.25	561.05	699.47	28.516	564.2	710.3	28.957	572.94
	2	471.16	520.5	277.22	473.81	70.256	278.77	481.14	71.343	283.09
	3	153.32	216.38	69.383	154.18	121.19	69.773	156.57	123.06	70.853
	4	90.11	143.67	38.091	90.623	176.3	38.305	92.026	179.03	38.898
	5	48.652	87.88	19.519	48.925	232.59	19.629	49.682	236.19	19.932

Table 8 Clamped-clamped frequencies (Hz) against height-radius ratio  $h/R$ 

	$h/R$	$q=0.5$			$q=1$			$q=8$		
		S-S	C-C	C-F	S-S	C-C	C-F	S-S	C-C	C-F
Category -I	0.001	13.213	28.292	5.052	13.142	28.141	5.025	12.95	27.73	4.952
	0.003	13.212	28.292	5.052	13.141	28.14	5.024	12.95	27.729	4.951
	0.006	13.211	28.291	5.051	13.14	28.14	5.024	12.949	27.729	4.951
	0.01	13.21	28.291	5.05	13.138	28.139	5.022	12.947	27.728	4.95
	0.03	13.203	28.288	5.047	13.127	28.135	5.017	12.941	27.726	4.946
Category -II	0.001	13.257	28.356	5.056	13.332	28.516	5.085	13.538	28.957	5.163
	0.003	13.258	28.357	5.057	13.333	28.516	5.085	13.539	28.957	5.164
	0.006	13.259	28.357	5.057	13.335	28.517	5.086	13.54	28.958	5.164
	0.01	13.261	28.358	5.058	13.337	28.518	5.087	13.541	28.959	5.165
	0.03	13.269	28.363	5.063	13.348	28.525	5.094	13.549	28.964	5.169

### 3.1 Frequency analysis of FGM cylindrical shells without ring supports

Here, the frequencies for FG-CS are evaluated with exponential volume fraction law under clamped-clamped (C-C), clamped-free (C-F) and simply supported - simply supported (SS-SS). Table 5 display FG-CS frequencies for Category I and Category II with the end conditions of C-C under exponential volume fraction. In this Table  $n$  is increased almost two times as compared to the edge condition of SS-SS at the initial value of  $n$  but almost its values becomes similar at  $n=5$ . The influence of the value of  $q$ , on both categories is same as it was seen for the end condition of SS-SS. Table 6 depicts the frequencies of FG-CSs versus the axial wave number for clamped-clamped conditions. The frequency increases on increasing the wave number and on increasing the value of  $q$  (0.5~8), the frequency decreases for all boundary conditions. It is observed that the frequencies of Category-II are greater than that of Category-I. It is due to the material which is used in the formation of shell.

Tables 7-8 shows the variations of clamped - clamped frequencies versus the  $L/R$  and  $h/R$  for FG-CS. In these tables, a great influence of ' $q$ ' has been seen on the variation of natural frequency. The affect of the value of ' $q$ ' is varied according to the Category I and Category II. In Table 8, it has been seen that there is a little bit changed when the value of  $L/R$  goes to higher step by step in both categories (I & II). For Category I and Category II the influence of the value of  $q$ , in the present case is similar Table 7.

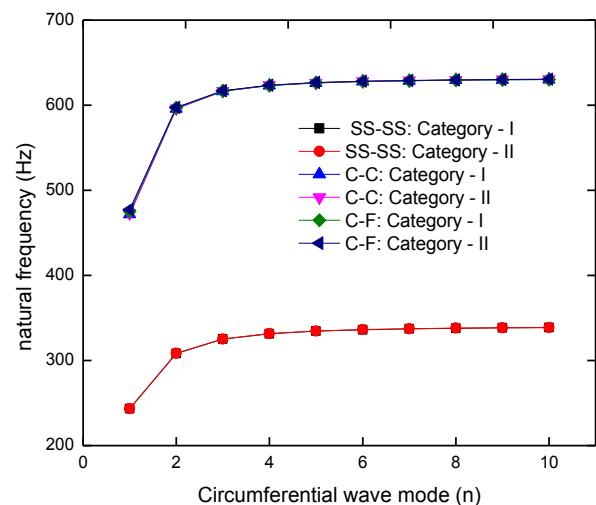


Fig. 2 Frequency pattern versus  $n$  for three boundary conditions for FG-CS with ring support ( $m=1$ ,  $L=20$  m,  $h=0.002$  m,  $R=1$  m,  $q=0.5$ ,  $a=0.3L$ )

### 3.2 Frequency analysis with ring supports

Here frequencies for both types of FG-CSs with ring supports are presented in following figures. The frequency variation with the position of the ring support at  $a=0.3L$  for the edge conditions: SS- SS, C-C and C-F for both FG-CS as shown in Fig. 2. The frequencies increase significantly from  $n=1$ ~10 and for other wave number, the frequencies increase linearly. Fig. 3. depicts the frequency variations versus ring support for Categories-I and-II cylindrical



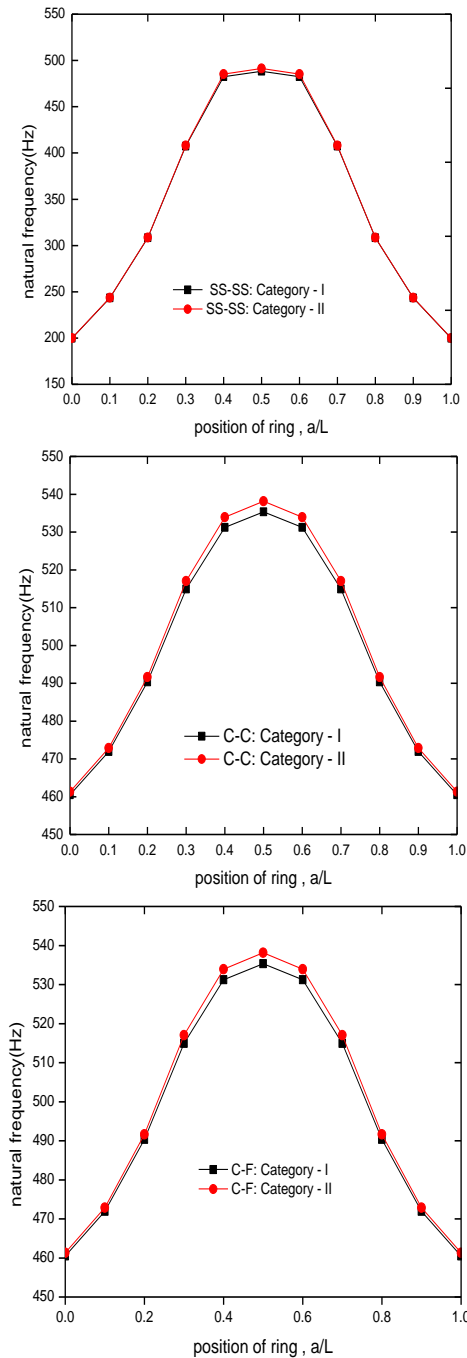


Fig. 3 Variations of frequencies versus the ring support  $a/L$  under various boundary conditions for FGM cylindrical shells ( $m=1$ ,  $n=1$ ,  $L=20$  m,  $h=0.002$  m,  $R=1$  m,  $q=0.5$ )

shells. These variations of frequencies are drawn with three types of end conditions. As  $a/L$  is enhanced for these boundary conditions, the frequencies go up. At  $a/L (=0.5)$  all the frequencies are higher and at  $a/L (=0.6-0.9)$ , the frequencies decrease. The frequencies are same at  $a/L=0, 1$  and rust itself a bell shape. In these figure, the C-F are lower than that of C-C and SS-SS. As shown by this figure, the boundary conditions C-C have the highest frequency curves. These frequencies have a great impact on the vibration of FG-CSs. It is inferred this frequency behavior with position of the ring supports has paramount influence

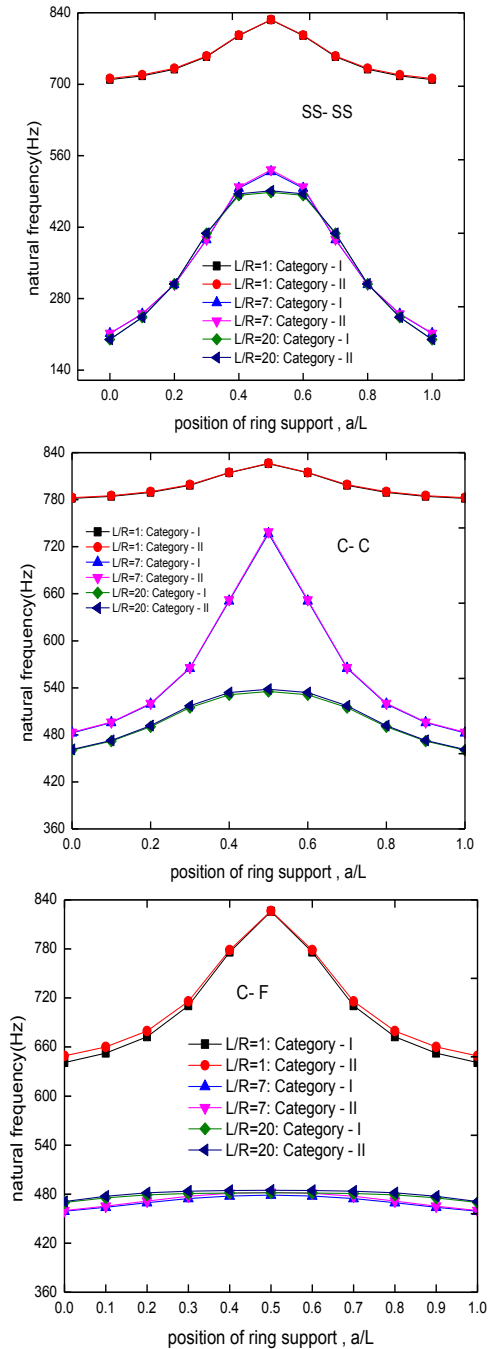
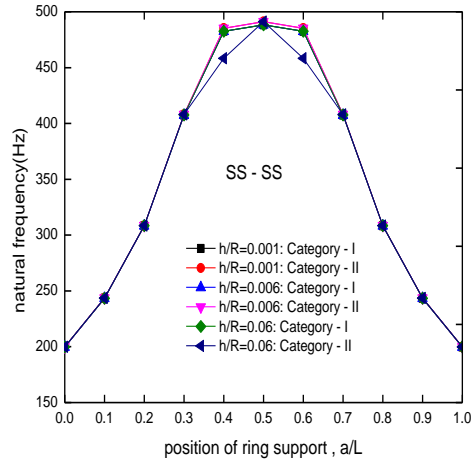
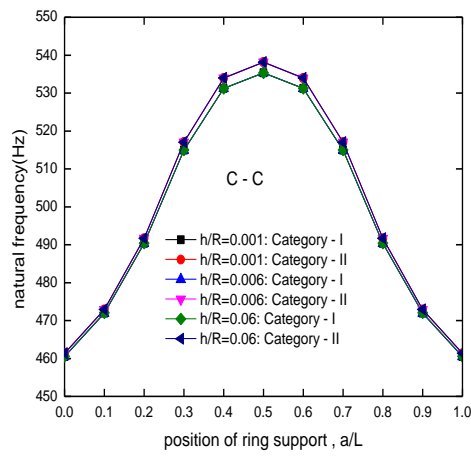


Fig. 4 Frequency variations at different ratios of  $L/R$  of FG-CSs with the position of ring support ( $n=1$ ,  $m=1$ ,  $h=0.002$  m,  $R=1$  m,  $q=0.5$ )

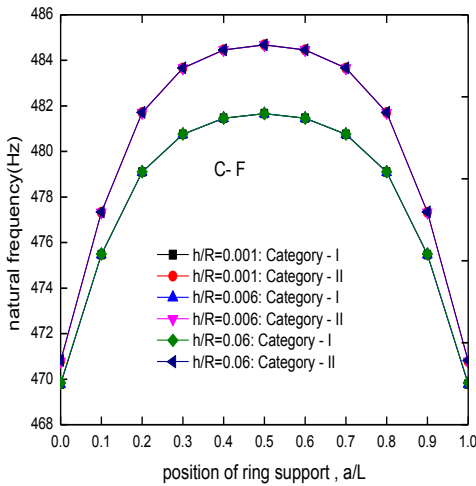
on the vibrations of FG-CSs. In Figs. 4 (a), (b), (c), frequencies for C-I and-II FG-CSs are sketched versus with position  $a$  of ring supports for three values of  $L/R=1, 7, 20$ . These results have been evaluated for three boundary conditions, respectively. Their graphical view presents that affect of ring support positions on vibration frequencies is pronounced at large values of  $L/R$  ratios where at  $L/R=1$ , their influence is reduced. Fig. 5 (a), (b), (c) demonstrate the frequencies of FG-CSs with three different boundary conditions against positions of ring supports. Frequency variations for these boundary conditions have observed



(a)



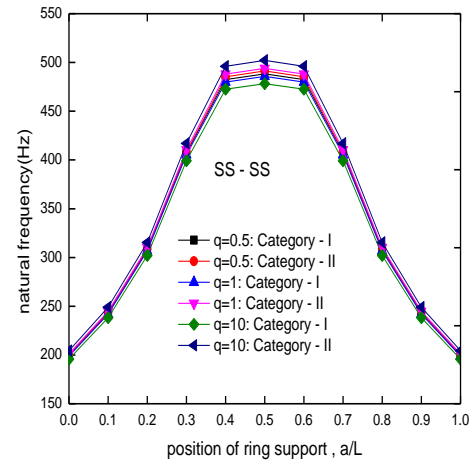
(b)



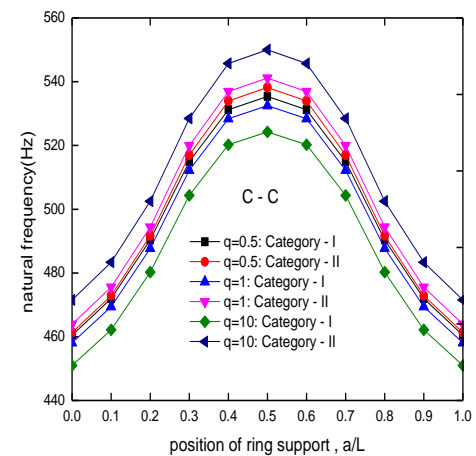
(c)

Fig. 5 Variations of frequencies at different ratios of  $h/R$  of FGM cylindrical shells with the position of ring supports.

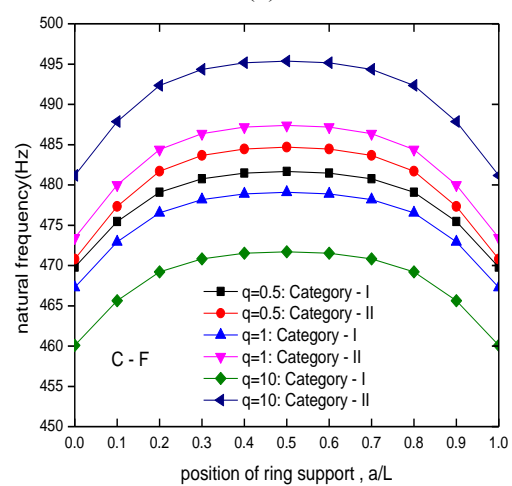
slightly different with parameter ( $L=20$ ,  $R=1$  m,  $q=0.5$ ). The SS-SS, C-C, C-F frequencies increase and decrease symmetrically around the mid location of ring supports. For rest of two end conditions, the variations of frequencies are observed to in linear style. Fig. 6 (a), (b), (c) depict the frequencies of FG-CS for Category-I and category-II cylindrical shells with specified boundary conditions. These



(a)



(b)



(c)

Fig. 6 Frequency variations different exponents of FGM cylindrical shells ( $n=1$ ,  $m=1$ ,  $L=20$  m,  $h=0.002$  m,  $R=1$  m)

variations have been plotted against the locations of ring supports for three values of exponents of volume fraction law. For three conditions, frequency variations show different behavior with these values of this law. The frequencies are visible for simply supported condition in the case of ring supports. The frequency first increases and gain maximum value in the midway of the shell length and then

lowers down. For clamped-clamped conditions, variations of frequencies are also like that for simply supported end conditions. For clamped-free conditions, frequency variations appear to be seen linear manner. For simply supported-simply supported conditions, a symmetrical behavior for natural frequencies is seen with the mid location of ring supports. For clamped-free conditions, a linear behavior of frequency variations is observed around the mid location of the ring supports.

#### 4. Conclusions

In this paper, utilizing the Love shell theory with exponential volume fraction laws for the CSs vibrations provides a governing equation for the distribution of material composition of material. It is also exhibited that the effect of frequencies by varying the positions of ring supports and ratios of length and height-to-radius. Effects of different parameters for ratios of length- and height-to-radius versus fundamental natural frequencies been determined for two categories of cylindrical shells. Throughout the computation, frequency behavior for the boundary condition follow as; C-C, SS-SS frequency curves are higher than that of C-F curves. Also the Love shell model based on the Galerkin's method for estimating fundamental natural frequency has been developed to converge more quickly than other methods and models. In addition, by increasing the value of height-to-radius ratio resulting frequencies also increase and frequencies decrease on increasing the ratio of length-to-radius ratio. For FG-CSs, variations of frequencies with the locations of ring supports have been analyzed placed round the circumferential direction. The position of a ring support has been taken along the radial direction. As the position of ring is enhanced for these boundary conditions, the frequencies go up. At mid point, all the frequencies are higher and after that the frequencies decreases. The frequencies are same at initial and final stage and rust itself a bell shape. Due to FG material ordering the increment and decrement frequencies occurs. For future work, this paper can be extended for the fluid-filled rotating of carbon nanotubes with ring supports.

#### Reference

- Alazzawy, W.I. and Jweeg, M.J. (2010), "A study of free vibration and fatigue for cross-ply closed cylindrical shells using General Third shell Theory (GTT)", *J. Eng.*, **16**(2), 5170-5184.
- Amabili, M., Pellicano, F. and Paidoussis, M.P. (1998), "Nonlinear vibrations of simply Love, A.E.H. (1888), 'On the small free vibrations and deformation of thin elastic shell'", *Phil. Tran. R. Soc. London*, **A179**, 491-549.
- Ansari, R. and Rouhi, H. (2015), "Nonlocal Flügge shell model for the axial buckling of single-walled Carbon nanotubes: An analytical approach", *Int. J. Nano Dimens.*, **6**(5), 453-462.
- Arshad, S.H., Naeem, M.N. and Sultana, N. (2007), "Frequency analysis of functionally graded cylindrical shells with various volume fraction laws", *J. Mech. Eng. Sci.*, **221**, 1483-1495. <https://doi.org/10.1243/09544062JMES738>.
- Asghar, S., Hussain, M. and Naeem, M. (2019), "Non-local effect on the vibration analysis of double walled carbon nanotubes based on Donnell shell theory", *Physica E: Low Dimens. Syst. Nanostruct.*, **116**, 113726. <https://doi.org/10.1016/j.physe.2019.113726>.
- Ayat, H., Kellouche, Y., Ghrici, M. and Boukhatem, B. (2018), "Compressive strength prediction of limestone filler concrete using artificial neural networks", *Adv. Comput. Des.*, **3**(3), 289-302. <https://doi.org/10.12989/acd.2018.3.3.289>.
- Batou, B., Nebab, M., Bennai, R., Atmane, H.A., Tounsi, A. and Bouremana, M. (2019), "Wave dispersion properties in imperfect sigmoid plates using various HSDTs", *Steel Compos. Struct.*, **33**(5), 699-716. <https://doi.org/10.12989/scs.2019.33.5.699>.
- Behera, S. and Kumari, P. (2018), "Free vibration of Levy-type rectangular laminated plates using efficient zig-zag theory", *Adv. Comput. Des.*, **3**(3), 213-232. <https://doi.org/10.12989/acd.2018.3.3.213>.
- Bilouei, B.S., Kolahchi, R. and Bidgoli, M.R. (2016), "Buckling of concrete columns retrofitted with Nano-Fiber Reinforced Polymer (NFRP)", *Comput. Concrete*, **18**(5), 1053-1063. <https://doi.org/10.12989/cac.2016.18.5.1053>.
- Chi, S.H. and Chung, Y.L. (2006), "Mechanical behavior of functionally graded material plates under transverse load-part II: numerical results", *Int. J. Solid. Struct.*, **43**, 3657-3691. <https://doi.org/10.1016/j.ijsolstr.2005.04.010>.
- Chung, H., Turula, P., Mulcahy, T.M. and Jendrzeczyk, J.A. (1981), "Analysis of cylindrical shell vibrating in a cylindrical fluid region", *Nucl. Eng. Des.*, **63**(1), 109-1012. [https://doi.org/10.1016/0029-5493\(81\)90020-0](https://doi.org/10.1016/0029-5493(81)90020-0).
- Dong, S.B. (1977), "A block-stodola eigen solution technique for large algebraic systems with non-symmetrical matrices", *Int. J. Numer. Meth. Eng.*, **11**, 247. <https://doi.org/10.1002/nme.1620110204>.
- Ergin, A. and Temarel, P. (2002), "Free vibration of a partially liquid-filled and submerged, horizontal cylindrical shell", *J. Sound Vib.*, **254**(5), 951-965. <https://doi.org/10.1006/jsvi.2001.4139>.
- Esmaeili, J. and Andalibia, K. (2019), "Development of 3D Meso-Scale finite element model to study the mechanical behavior of steel microfiber-reinforced polymer concrete", *Comput. Concrete*, **24**(5), 413-422. <https://doi.org/10.12989/cac.2019.24.5.413>.
- Fatahi-Vajari, A., Azimzadeh, Z. and Hussain, M. (2019), "Nonlinear coupled axial-torsional vibration of single-walled carbon nanotubes using Galerkin and Homotopy perturbation method", *Micro Nano Lett.*, **14**(14), 1366-1371. <https://doi.org/10.1049/mnl.2019.0203>.
- Gasser, T.C. (2007), "Validation of 3D crack propagation in plain concrete. Part II: Computational modeling and predictions of the PCT3D test", *Comput. Concrete*, **4**(1), 67-82. <https://doi.org/10.12989/cac.2007.4.1.067>.
- Ghodrati, B., Yaghootian, A., Ghanbar Zadeh, A. and Mohammad-Sedighi, H. (2018), "Lamb wave extraction of dispersion curves in micro/nano-plates using couple stress theories", *Wave. Rand. Complex Media*, **28**(1), 15-34. <https://doi.org/10.1080/17455030.2017.1308582>.
- Golabchi, H., Kolahchi, R. and Bidgoli, M.R. (2018), "Vibration and instability analysis of pipes reinforced by SiO<sub>2</sub> nanoparticles considering agglomeration effects", *Comput. Concrete*, **21**(4), 431-440. <https://doi.org/10.12989/cac.2018.21.4.431>.
- Goncalves, P.B. and Batista, R.C. (1988), "Non-linear vibration analysis of fluid-filled cylindrical shells", *J. Sound Vib.*, **127**(1), 133-143. [https://doi.org/10.1016/0022-460X\(88\)90354-9](https://doi.org/10.1016/0022-460X(88)90354-9).
- Greif, R. and Chung, H. (1975), "Vibration of constrained cylindrical shells", *Am. Inst. Aeronaut. J.*, **13**, 1190-1198. <https://doi.org/10.2514/3.6970>.
- Hussain, M. and Naeem, M. (2017), "Vibration analysis of single-walled carbon nanotubes using wave propagation approach", *Mech. Sci.*, **8**(1), 155-164. <https://doi.org/10.5194/ms-8-155-2017>.

- Hussain, M. and Naeem, M. (2018), "Vibration of single-walled carbon nanotubes based on Donnell shell theory using wave propagation approach", Chapter, Intechopen, Novel Nanomaterials - Synthesis and Applications, ISBN 978-953-51-5896-7. <https://doi.org/10.5772/intechopen.73503>.
- Hussain, M. and Naeem, M. (2018a), "Vibration of single-walled carbon nanotubes based on Donnell shell theory using wave propagation approach", Chapter, Intechopen, Novel Nanomaterials - Synthesis and Applications, ISBN 978-953-51-5896-7. <https://doi.org/10.5772/intechopen.73503>.
- Hussain, M. and Naeem, M. (2019a), "Vibration characteristics of single-walled carbon nanotubes based on non-local elasticity theory using wave propagation approach (WPA) including chirality", Perspective of Carbon Nanotubes. IntechOpen. <https://doi.org/10.5772/intechopen.85948>.
- Hussain, M. and Naeem, M. (2019d), "Rotating response on the vibrations of functionally graded zigzag and chiral single walled carbon nanotubes", *Appl. Math. Model.*, **75**, 506-520. <https://doi.org/10.1016/j.apm.2019.05.039>.
- Hussain, M. and Naeem, M.N. (2017), "Vibration analysis of single-walled carbon nanotubes using wave propagation approach", *Mech. Sci.*, **8**(1), 155-164. <https://doi.org/10.5194/ms-8-155-2017>.
- Hussain, M. and Naeem, M.N. (2018b), "Effect of various edge conditions on free vibration characteristics of rectangular plates", Chapter, Intechopen, Advance Testing and Engineering, ISBN 978-953-51-6706-8, Intechopen.
- Hussain, M. and Naeem, M.N. (2019b), "Effects of ring supports on vibration of armchair and zigzag FGM rotating carbon nanotubes using Galerkin's method", *Compos. Part B. Eng.*, **163**, 548-561. <https://doi.org/10.1016/j.compositesb.2018.12.144>.
- Hussain, M. and Naeem, M.N. (2019c), "Vibration characteristics of zigzag and chiral FGM rotating carbon nanotubes sandwich with ring supports", *J. Mech. Eng. Sci., Part C*, **233**(16), 5763-5780. <https://doi.org/10.1177/0954406219855095>.
- Hussain, M. and Naeem, M.N. (2020a), "Mass density effect on vibration of zigzag and chiral SWCNTs", *J. Sandw. Struct. Mater.*, 1099636220906257. <https://doi.org/10.1177/1099636220906257>.
- Hussain, M. and Naeem, M.N. (2020b), "Vibration characteristics of zigzag FGM single-walled carbon nanotubes based on Ritz method with ring-stiffeners", *Ind. J. Phys.*, **140**, 85-98. <https://doi.org/10.1016/j.tws.2019.03.018>.
- Hussain, M., Naeem, M., Shahzad, A. and He, M. (2017), "Vibrational behavior of single-walled carbon nanotubes based on cylindrical shell model using wave propagation approach", *AIP Adv.*, **7**(4), 045114. <https://doi.org/10.1063/1.4979112>.
- Hussain, M., Naeem, M., Shahzad, A. and He, M. (2018a), "Vibration characteristics of fluid-filled functionally graded cylindrical material with ring supports", Chapter, Intechopen, Computational Fluid Dynamics, ISBN 978-953-51-5706-9, <https://doi.org/10.5772/intechopen.72172>.
- Hussain, M., Naeem, M.N. and Isvandzibaei, M. (2018c), "Effect of Winkler and Pasternak elastic foundation on the vibration of rotating functionally graded material cylindrical shell", *Proc. Inst. Mech. Eng., Part C: J. Mech. Eng. Sci.*, **232**(24), 4564-4577. <https://doi.org/10.1177/0954406217753459>.
- Hussain, M., Naeem, M.N. and Taj, M. (2019b), "Effect of length and thickness variations on the vibration of SWCNTs based on Flügge's shell model", *Micro Nano Lett.*, <https://doi.org/10.1049/mnl.2019.0309>.
- Hussain, M., Naeem, M.N. and Tounsi, A. (2020a), "Simulating vibration of single-walled carbon nanotube based on Relagh-Ritz Method".
- Hussain, M., Naeem, M.N. and Tounsi, A. (2020b), "On mixing the Rayleigh-Ritz formulation with Hankel's function for vibration of fluid-filled Fluid-filled cylindrical shell", *Adv. Comput. Des.*, (in Press)
- Hussain, M., Naeem, M.N. and Tounsi, A. (2020c), "Numerical Study for nonlocal vibration of orthotropic SWCNTs based on Kelvin's model", *Adv. Concrete Constr.*, **9**(3), 301-312. <https://doi.org/10.12989/acc.2020.9.3.301>.
- Hussain, M., Naeem, M.N. and Tounsi, A. (2020d), "Response of orthotropic Kelvin modeling for single-walled carbon nanotubes: Frequency analysis", *Adv. Nano Res.*, **8**(3). (in Press)
- Hussain, M., Naeem, M.N. and Tounsi, A. (2020e), "Theoretical impact of Kelvin's theory for vibration of double walled carbon nanotubes", *Advance Nano Research*. (submitted)
- Hussain, M., Naeem, M.N., Sehar, A. and Tounsi, A. (2020g), "Eringen's nonlocal model sandwich with Kelvin's theory for vibration of DWCNT", *Comput. Concrete*, **25**(4). (in Press)
- Hussain, M., Naeem, M.N., Shahzad, A., He, M. and Habib, S. (2018b), "Vibrations of rotating cylindrical shells with FGM using wave propagation approach", *IMEchE Part C: J. Mech. Eng. Sci.*, **232**(23), 4342-4356.
- Hussain, M., Naeem, M.N., Tounsi, A. and Taj, M. (2019a), "Nonlocal effect on the vibration of armchair and zigzag SWCNTs with bending rigidity", *Adv. Nano Res.*, **7**(6), 431-442. <https://doi.org/10.12989/anr.2019.7.6.431>.
- Hussain, M., Naeem, M.N., Shahzad, A. and He, M. (2017), "Vibrational behavior of single-walled carbon nanotubes based on cylindrical shell model using wave propagation approach", *AIP Adv.*, **7**(4), 045114. <https://doi.org/10.1063/1.4979112>.
- Jamali, M., Shojaei, T., Mohammadi, B. and Kolahchi, R. (2019), "Cut out effect on nonlinear post-buckling behavior of FG-CNTRC micro plate subjected to magnetic field via FSDT", *Adv. Nano Res.*, **7**(6), 405-417. <https://doi.org/10.12989/anr.2019.7.6.405>.
- Jiang, J. and Olson, M.D. (1994), "Vibrational analysis of orthogonally stiffened cylindrical shells using super elements", *J. Sound Vib.*, **173**, 73-83. <https://doi.org/10.1006/jsvi.1994.1218>.
- Jweeg, M.J. and Alazzawy, W.I. (2007), "A suggested analytical solution for laminated closed cylindrical shells using General Third Shell Theory (GTT)", *Al-Nahrain J. Eng. Sci.*, **10**(1), 11-26.
- Koizumi, M. (1997), "FGM activities in Japan", *Compos. Part B: Eng.*, **28**(1-2), 1-4.
- Lal, A. and Markad, K. (2018), "Deflection and stress behaviour of multi-walled carbon nanotube reinforced laminated composite beams", *Comput. Concrete*, **22**(6), 501-514. <https://doi.org/10.12989/cac.2018.22.6.501>.
- Lam, K.Y. and Loy, C.T. (1998), "Influence of boundary conditions for a thin laminated rotating cylindrical shell", *Compos. Struct.*, **41**, 215-228. [https://doi.org/10.1016/S0263-8223\(98\)00012-9](https://doi.org/10.1016/S0263-8223(98)00012-9).
- Loghman, A., Arani, A.G. and Barzoki, A.A.M. (2017), "Nonlinear stability of non-axisymmetric functionally graded reinforced nano composite microplates", *Comput. Concrete*, **19**(6), 677-687. <https://doi.org/10.12989/cac.2017.19.6.677>.
- Loy, C.T. and Lam, K.Y. (1997), "Vibration of cylindrical shells with ring supports", *J. Mech. Eng.*, **39**, 455-471. [https://doi.org/10.1016/S0020-7403\(96\)00035-5](https://doi.org/10.1016/S0020-7403(96)00035-5).
- Loy, C.T., Lam, K.Y. and Reddy, J.N. (1999), "Vibration of functionally graded cylindrical shells", *Int. J. Mech. Sci.*, **41**, 309-324. [https://doi.org/10.1016/S0020-7403\(98\)00054-X](https://doi.org/10.1016/S0020-7403(98)00054-X).
- Mahapatra, T.R., Kar, V.R., Panda, S.K. and Mehar, K. (2017), "Nonlinear thermoelastic deflection of temperature-dependent FGM curved shallow shell under nonlinear thermal loading", *J. Therm. Stress.*, **40**(9), 1184-1199. <https://doi.org/10.1080/01495739.2017.1302788>.
- Meftah, S.A., Tounsi, A. and Adda Bedia, E.A. (2006), "Dynamic behaviour of stiffened and damaged coupled shear walls"

- Comput. Concrete*, **3**(5), 1-15. <https://doi.org/10.12989/cac.2006.3.5.285>.
- Mehar, K. and Kumar Panda, S. (2018), "Thermal free vibration behavior of FG-CNT reinforced sandwich curved panel using finite element method", *Polym. Compos.*, **39**(8), 2751-2764. <https://doi.org/10.1002/pc.24266>.
- Mehar, K. and Panda, S.K. (2016), "Geometrical nonlinear free vibration analysis of FG-CNT reinforced composite flat panel under uniform thermal field", *Compos. Struct.*, **143**, 336-346. <https://doi.org/10.1016/j.compstruct.2016.02.038>.
- Mehar, K. and Panda, S.K. (2017a), "Numerical investigation of nonlinear thermomechanical deflection of functionally graded CNT reinforced doubly curved composite shell panel under different mechanical loads", *Compos. Struct.*, **161**, 287-298. <https://doi.org/10.1016/j.compstruct.2016.10.135>.
- Mehar, K. and Panda, S.K. (2017b), "Thermoelastic analysis of FG-CNT reinforced shear deformable composite plate under various loadings", *Int. J. Comput. Meth.*, **14**(2), 1750019. <https://doi.org/10.1142/S0219876217500190>.
- Mehar, K. and Panda, S.K. (2017d), "Nonlinear static behavior of FG-CNT reinforced composite flat panel under thermomechanical load", *J. Aerosp. Eng.*, **30**(3), 04016100. [https://doi.org/10.1061/\(ASCE\)AS.1943-5525.0000706](https://doi.org/10.1061/(ASCE)AS.1943-5525.0000706).
- Mehar, K. and Panda, S.K. (2019), "Multiscale modeling approach for thermal buckling analysis of nanocomposite curved structure", *Adv. Nano Res.*, **7**(3), 181. <https://doi.org/10.12989/anr.2019.7.3.181>.
- Mehar, K., Mishra, P.K. and Panda, S.K. (2020b), "Numerical investigation of thermal frequency responses of graded hybrid smart nanocomposite (CNT-SMA-Epoxy) structure", *Mech. Adv. Mater. Struct.*, 1-13. <https://doi.org/10.1080/15376494.2020.1725193>.
- Mehar, K., Panda, S.K. and Mahapatra, T.R. (2017a), "Thermoelastic nonlinear frequency analysis of CNT reinforced functionally graded sandwich structure", *Eur. J. Mech.-A/Solid.*, **65**, 384-396. <https://doi.org/10.1016/j.euromechsol.2017.05.005>.
- Mehar, K., Panda, S.K. and Mahapatra, T.R. (2017c), "Theoretical and experimental investigation of vibration characteristic of carbon nanotube reinforced polymer composite structure", *Int. J. Mech. Sci.*, **133**, 319-329. <https://doi.org/10.1016/j.ijmecsci.2017.08.057>.
- Mehar, K., Panda, S.K. and Mahapatra, T.R. (2017d), "Theoretical and experimental investigation of vibration characteristic of carbon nanotube reinforced polymer composite structure", *Int. J. Mech. Sci.*, **133**, 319-329. <https://doi.org/10.1016/j.ijmecsci.2017.08.057>.
- Mehar, K., Panda, S.K. and Patle, B.K. (2018), "Stress, deflection, and frequency analysis of CNT reinforced graded sandwich plate under uniform and linear thermal environment: A finite element approach", *Polym. Compos.*, **39**(10), 3792-3809. <https://doi.org/10.1002/pc.24409>.
- Mehar, K., Panda, S.K. and Sharma, N. (2020a), "Numerical investigation and experimental verification of thermal frequency of carbon nanotube-reinforced sandwich structure", *Eng. Struct.*, **211**, 110444. <https://doi.org/10.1016/j.engstruct.2020.110444>.
- Mehar, K., Panda, S.K., Bui, T.Q. and Mahapatra, T.R. (2017b), "Nonlinear thermoelastic frequency analysis of functionally graded CNT-reinforced single/doubly curved shallow shell panels by FEM", *J. Therm. Stress.*, **40**(7), 899-916. <https://doi.org/10.1080/01495739.2017.1318689>.
- Mehar, K., Panda, S.K., Dehengia, A. and Kar, V.R. (2016), "Vibration analysis of functionally graded carbon nanotube reinforced composite plate in thermal environment", *J. Sandw. Struct. Mater.*, **18**(2), 151-173. <https://doi.org/10.1177/1099636215613324>.
- Mehar, K., Panda, S.K., Devarajan, Y. and Choubey, G. (2019), "Numerical buckling analysis of graded CNT-reinforced composite sandwich shell structure under thermal loading", *Compos. Struct.*, **216**, 406-414. <https://doi.org/10.1016/j.compstruct.2019.03.002>.
- Mousavi, M., Mohammadimehr, M. and Rostami, R. (2019), "Analytical solution for buckling analysis of micro sandwich hollow circular plate", *Comput. Concrete*, **24**(3), 185-192. <https://doi.org/10.12989/cac.2019.24.3.185>.
- Naeem, M.N., Ghamkhar, M., Arshad, S.H. and Shah, A.G. (2013), "Vibration analysis of submerged thin FGM cylindrical shells", *J. Mech. Sci. Technol.*, **27**(3), 649-656. <https://doi.org/10.1007/s12206-013-0119-6>.
- Najafizadeh, M.M. and Isvandzibaei, M.R. (2007), "Vibration of (FGM) cylindrical shells based on higher order shear deformation plate theory with ring support", *Acta Mechanica*, **191**, 75-91. <https://doi.org/10.1007/s00707-006-0438-0>.
- Najafizadeh, M.M. and Isvandzibaei, M.R. (2009), "Vibration of functionally graded cylindrical shells based on different shear deformation shell theories with ring support under various boundary conditions", *J. Mech. Sci. Technol.*, **23**(8), 2072-2084. <https://doi.org/10.1007/s12206-009-0432-2>.
- Narwariya, M., Choudhury, A. and Sharma, A.K. (2018), "Harmonic analysis of moderately thick symmetric cross-ply laminated composite plate using FEM", *Adv. Comput. Des.*, **3**(2), 113-132. <https://doi.org/10.12989/acd.2018.3.2.113>.
- Rezaiee-Pajand, M., Masoodi, A.R. and Mokhtari, M. (2018), "Static analysis of functionally graded non-prismatic sandwich beams", *Adv. Comput. Des.*, **3**(2), 165-190. <https://doi.org/10.12989/acd.2018.3.2.165>.
- Salah, F., Boucham, B., Bourada, F., Benzair, A., Bousahla, A.A. and Tounsi, A. (2019), "Investigation of thermal buckling properties of ceramic-metal FGM sandwich plates using 2D integral plate model", *Steel Compos. Struct.*, **32**(5), 595-610. <https://doi.org/10.12989/scs.2019.33.6.805>.
- Salamat, D. and Sedighi, H.M. (2017), "The effect of small scale on the vibrational behavior of single-walled carbon nanotubes with a moving nanoparticle", *J. Appl. Comput. Mech.*, **3**(3), 208-217. <https://doi.org/10.22055/JACM.2017.12740>.
- Sedighi, H.M. and Sheikhanzadeh, A.S.H.K.A.N. (2017), "Static and dynamic pull-in instability of nano-beams resting on elastic foundation based on the nonlocal elasticity theory", *Chin. J. Mech. Eng.*, **30**(2), 385-397. <https://doi.org/10.1007/s10033-017-0079-3>.
- Sedighi, H.M., Reza, A. and Zare, J. (2011), "Study on the frequency-amplitude relation of beam vibration", *Int. J. Phys. Sci.*, **6**(36), 8051-8056. <https://doi.org/10.5897/IJPS11.1556>.
- Sewall, J.L. and Naumann, E.C. (1968), "An experimental and analytical vibration study of thin cylindrical shells with and without longitudinal stiffeners", National Aeronautic and Space Administration, the Clearinghouse for Federal Scientific and Technical Information, Springfield, VA..
- Shah, A.G., Mahmood, T. and Naeem, M.N. (2009), "Vibrations of FGM thin cylindrical shells with exponential volume fraction law", *Appl. Math. Mech.*, **30**(5), 607-615. <https://doi.org/10.1007/s10483-009-0507-x>.
- Sharma, C.B. and Johns, D.J. (1971), "Vibration characteristics of a clamped-free and clamped-ring-stiffened circular cylindrical shell", *J. Sound Vib.*, **14**(4), 459-474. [https://doi.org/10.1016/0022-460X\(71\)90575-X](https://doi.org/10.1016/0022-460X(71)90575-X).
- Sharma, C.B., Darvizeh, M. and Darvizeh, A. (1998), "Natural frequency response of vertical cantilever composite shells containing fluid", *Eng. Struct.*, **20**(8), 732-737. [https://doi.org/10.1016/S0141-0296\(97\)00102-8](https://doi.org/10.1016/S0141-0296(97)00102-8).
- Sharma, P., Singh, R. and Hussain, M. (2019), "On modal analysis of axially functionally graded material beam under hygrothermal effect", *Proc. Inst. Mech. Eng., Part C: J. Mech. Eng. Sci.*, **234**(5), 1085-1101.

- <https://doi.org/10.1177/0954406219888234>.
- Sharma, P., Singh, R., Hussain, M. (2019), "On modal analysis of axially functionally graded material beam under hygrothermal effect", *Proc. Inst. Mech. Eng., Part C: J. Mech. Eng. Sci.*, **234**(5), 1085-1101. <https://doi.org/10.1177/0954406219888234>.
- Sodel, W. (1981), *Vibration of Shell and Plates, Mechanical Engineering Series*, Marcel Dekker, New York.
- Sofiyev, A.H. and Avcar, M. (2010), "The stability of cylindrical shells containing an FGM layer subjected to axial load on the Pasternak foundation", *Eng.*, **2**(4), 228. <https://doi.org/10.4236/eng.2010.24033>.
- Suresh, S. and Mortensen, A. (1997), "Functionally gradient metals and metal ceramic composites, Part 2: Thermo Mechanical Behavior", *Int. Mater.*, **42**, 85-116. <https://doi.org/10.1179/imr.1997.42.3.85>.
- Swaddiwudhipong, S., Tian, J. and Wang, C.M. (1995), "Vibrations of cylindrical shells with intermediate supports", *J. Sound Vib.*, **187**, 69-93. <https://doi.org/10.1006/jsvi.1995.0503>.
- Taj, M., Hussain, M., Naeem, M.N. and Tounsi, A. (2020c), "Effects of elastic medium on buckling of microtubules due to bending and torsion", *Advances in Concrete Construction*. (submitted)
- Taj, M., Safeer, M., Hussain, M., Naeem, M.N., Ahmad, M., Abbas, K., Khan, A.Q. and Tounsi, A. (2020b), "A effect of external force on cytoskeleton components in viscoelastic media", *Computers and Concrete*. (submitted)
- Taj, M., Safeer, M., Hussain, M., Naeem, M.N., Majeed, A., Ahmad, M., Khan, H.U. and Tounsi, A. (2020a), "Non-local orthotropic elastic shell model for vibration analysis of protein microtubules", *Comput. Concrete*, **25**(3), 245-253. <https://doi.org/10.12989/cac.2020.25.3.245>
- Thomé, B., Schikora, K. and Bletzinger, K.U. (2006), "Material modeling of steel fiber reinforced concrete", *Comput. Concrete*, **3**(4), 197-212. <https://doi.org/10.12989/cac.2006.3.4.197>.
- Touloukian, Y.S. (1967), *Thermo Physical Properties of High Temperature Solid Materials*, Macmillan, New York.
- Wang, C. and Lai, J.C.S. (2000), "Prediction of natural frequencies of finite length circular cylindrical shells", *Appl. Acoust.*, **59**(4), 385-400. [https://doi.org/10.1016/S0003-682X\(99\)00039-0](https://doi.org/10.1016/S0003-682X(99)00039-0).
- Wang, C.M., Swaddiwudhipong, S. and Tian, J. (1997), "Ritz method for vibration analysis of cylindrical shells with ring-stiffeners", *J. Eng. Mech.*, **123**, 134-143. [https://doi.org/10.1061/\(ASCE\)0733-9399\(1997\)123:2\(134\)](https://doi.org/10.1061/(ASCE)0733-9399(1997)123:2(134)).
- Wuite, J. and Adali, S. (2005), "Deflection and stress behaviour of nanocomposite reinforced beams using a multiscale analysis", *Compos. Struct.*, **71**(3-4), 388-396. <https://doi.org/10.1016/j.compstruct.2005.09.011>.
- Xiang, Y., Ma, Y.F., Kitipornchai, S. and Lau, C.W.H. (2002), "Exact solutions for vibration of cylindrical shells with intermediate ring supports", *Int. J. Mech. Sci.*, **44**(9), 1907-1924. [https://doi.org/10.1016/S0020-7403\(02\)00071-1](https://doi.org/10.1016/S0020-7403(02)00071-1).
- Xuebin, L. (2008), "Study on free vibration analysis of circular cylindrical shells using wave propagation", *J. Sound Vib.*, **311**, 667-682. <https://doi.org/10.1016/j.jsv.2007.09.023>.
- Yaman, I.O., Akbay, Z. and Aktan, H. (2006), "Numerical modelling and finite element analysis of stress wave propagation for ultrasonic pulse velocity testing of concrete", *Comput. Concrete*, **3**(6), 423-437. <https://doi.org/10.12989/cac.2006.3.6.423>.
- Yazdani, R. and Mohammadimehr, M. (2019), "Double bonded Cooper-Naghdi micro sandwich cylindrical shells with porous core and CNTRC face sheets: Wave propagation solution", *Comput. Concrete*, **24**(6), 499-511. <https://doi.org/10.12989/cac.2019.24.6.499>.
- Zamani, A., Kolahchi, R. and Bidgoli, M.R. (2017), "Seismic response of smart nanocomposite cylindrical shell conveying fluid flow using HDQ-Newmark methods", *Comput. Concrete*, **20**(6), 671-682. <https://doi.org/10.12989/cac.2017.20.6.671>.
- Zhang, X.M. (2002), "Parametric analysis of frequency of rotating laminated composite cylindrical shells with the wave propagation approach", *Comput. Meth. Appl. Mech. Eng.*, **191**, 2057-2071. [https://doi.org/10.1016/S0045-7825\(01\)00368-1](https://doi.org/10.1016/S0045-7825(01)00368-1).

CC

## Appendix-I

$$\begin{aligned}
\lambda_{11} &= A_{11} \frac{\partial^2}{\partial x^2} + \left( \frac{A_{66}}{R^2} + \rho_t \right) \frac{\partial^2}{\partial \theta^2} \\
\lambda_{12} &= \frac{(A_{12} + A_{66})}{R} \frac{\partial^2}{\partial x \partial \theta} + \frac{(B_{12} + 2B_{66})}{R^2} \frac{\partial^2}{\partial x \partial \theta} \\
\lambda_{13} &= \left( \frac{A_{12}}{R} - \rho_t R \right) \frac{\partial}{\partial x} - B_{11} \frac{\partial^3}{\partial x^3} - \frac{(B_{12} + 2B_{66})}{R^2} \frac{\partial^3}{\partial x \partial \theta^2} \\
\lambda_{21} &= \left( \frac{A_{12} + A_{66}}{R} + \frac{B_{12} + B_{66}}{R^2} + \rho_t R \right) \frac{\partial^2}{\partial x \partial \theta} \\
\lambda_{22} &= \left( A_{66} + \frac{3B_{66}}{R} + \frac{2D_{66}}{R^2} \right) \frac{\partial^2}{\partial x^2} + \left( \frac{A_{22}}{R^2} + \frac{2B_{22}}{R^3} + \frac{D_{22}}{R^4} \right) \frac{\partial^2}{\partial \theta^2} + \rho_t \\
\lambda_{23} &= \left( \frac{A_{22}}{R^2} + \frac{B_{22}}{R^3} \right) \frac{\partial}{\partial \theta} - \left( \frac{B_{22}}{R^3} + \frac{D_{22}}{R^4} \right) \frac{\partial^3}{\partial \theta^3} \\
&\quad - \left( \frac{B_{12} + 2B_{66}}{R} + \frac{D_{12} + 2D_{66}}{R^2} \right) \frac{\partial^3}{\partial x^2 \partial \theta} - 2\rho_t \frac{\partial}{\partial t} \\
\lambda_{31} &= -\frac{A_{12}}{R} \frac{\partial}{\partial x} + B_{11} \frac{\partial^3}{\partial x^3} + \left( \frac{B_{12} + 2B_{66}}{R^2} \right) \frac{\partial^3}{\partial x \partial \theta^2} \\
\lambda_{32} &= -\left( \frac{A_{22}}{R^2} + \frac{B_{22}}{R^3} + \rho_t \right) \frac{\partial}{\partial \theta} + \left( \frac{B_{22}}{R^3} + \frac{D_{22}}{R^4} \right) \frac{\partial^3}{\partial \theta^3} \\
&\quad + \left( \frac{B_{12} + 2B_{66}}{R} + \frac{D_{12} + 4D_{66}}{R^2} \right) \frac{\partial^3}{\partial x^2 \partial \theta} + 2\rho_t \frac{\partial}{\partial t} \\
\lambda_{33} &= -\frac{A_{22}}{R^2} + \rho_t + \frac{2B_{12}}{R} \frac{\partial^2}{\partial x^2} + \left( \frac{2B_{22}}{R^3} + \rho_t \right) \frac{\partial^2}{\partial \theta^2} \\
&\quad - D_{11} \frac{\partial^4}{\partial x^4} - 2 \left( \frac{D_{12} + 2D_{66}}{R^2} \right) \frac{\partial^4}{\partial x^2 \partial \theta^2} - \frac{D_{22}}{R^4} \frac{\partial^4}{\partial \theta^4}
\end{aligned}$$

Where

$$\begin{aligned}
I_1 &= \int_0^L \frac{d^3 \psi}{dx^3} \frac{d\psi}{dx} dx \quad I_2 = \int_0^L \frac{d\psi}{dx} \frac{d\psi}{dx} dx \quad I_3 = \int_0^L \frac{d^2 \psi}{dx^2} \psi(x) dx \\
I_4 &= \int_0^L \psi(x) \psi(x) dx \quad I_5 = \int_0^L \frac{d^4 \psi}{dx^4} \psi(x) dx \quad I_6 = \int_0^L (x-a) \frac{d\psi}{dx} \frac{d\psi}{dx} dx \\
I_7 &= \int_0^L \psi(x) \frac{d\psi}{dx} dx \quad I_8 = \int_0^L (x-a) \frac{d^3 \psi}{dx^3} \frac{d\psi}{dx} dx \quad I_9 = \int_0^L \frac{d^2 \psi}{dx^2} \frac{d\psi}{dx} dx \\
I_{10} &= \int_0^L (x-a) \psi(x) \psi(x) dx \quad I_{11} = \int_0^L \frac{d^2 \psi}{dx^2} (x-a) \psi(x) dx \quad I_{12} = I_7 \\
I_{13} &= \int_0^L \psi^2(x) (x-a)^2 dx \quad I_{14} = \int_0^L \frac{d^2 \psi}{dx^2} \psi(x) (x-a)^2 dx \\
I_{15} &= \int_0^L \frac{d\psi}{dx} \psi(x) (x-a) dx \quad I_{16} = \int_0^L \frac{d^4 \psi}{dx^4} \psi(x) (x-a)^2 dx \\
I_{17} &= \int_0^L \frac{d^3 \psi}{dx^3} \psi(x) (x-a) dx \quad I_{18} = \int_0^L \frac{d^2 \psi}{dx^2} \psi(x) (x-a) dx \\
I_{19} &= \int_0^L \frac{d^4 \psi}{dx^4} \psi(x) (x-a) dx
\end{aligned}$$